

## Transition to chaos via sequences of border collision bifurcations in a single-phase power electronic inverter

Viktor Avrutin<sup>1,4</sup>, Zhanybai T. Zhusubaliyev<sup>2</sup>, Erik Mosekilde<sup>3</sup> and Laura Gardini<sup>4</sup>

<sup>1</sup> Institute for Systems Theory and Automatic Control, University of Stuttgart, Pfaffenwaldring 9, 70550 Stuttgart, Germany

<sup>2</sup> Department of Computer Science, South West State University, 50 Years of October Str., 94, 305040, Kursk, Russia

<sup>3</sup> Department of Physics, The Technical University of Denmark, Fysikvej 309, 2800 Lyngby, Denmark

<sup>4</sup> Department of Economics, Society and Politics, University of Urbino, Via Saffi 42, 61029 Urbino, Italy

Email: Viktor.Avrutin@ist.uni-stuttgart.de, Zhanybai@hotmail.com, Erik.Mosekilde@fysik.dtu.dk, Laura.Gardini@uniurb.it

**Abstract**—Power electronic DC/AC converters play an important role in modern power supply technology. As parameters are varied, such converters may display a variety of unusual phenomena caused by the interaction of two internal oscillatory modes (the ramp cycle and the external sinusoidal reference signal). In this paper we consider a non-autonomous piecewise-smooth map describing the behavior of a DC/AC power converter. The dynamics of the map are investigated using a one-dimensional autonomous stroboscopic map. We discuss a new type of complex dynamics in which chaotic oscillations appear through an unusual sequence of border collision bifurcations, differently from a well-known direct transition from a stable fixed point to chaos.

### 1. Introduction

Power electronic DC/AC converters (also known as inverters) [1, 2] provide AC power from a DC source. Converters of this type are used in backup systems for sensitive computers or hospital equipment and as so-called grid-tie inverters to convert low voltage DC power from a solar panel into AC power. Further applications of such converters include uninterruptible power supplies (UPS), active filters, flexible AC transmission systems (FACTS), voltage compensators, to list a few [1]. By contrast to DC/DC converters where the constant reference signal only changes in response to variations in the operational conditions, a DC/AC converter requires a sinusoidal reference signal that besides the amplitude of the desired output voltage (or current) also prescribes the frequency and phase of this output. This form of external forcing introduces an additional source of interaction between the low frequency power mode and the high frequency switching cycle, and this interaction gives birth to a variety of unusual nonlinear dynamic phenomena, including for example the recently reported phase synchronized quasiperiodicity [3, 4, 5].

The purpose of the present paper is to investigate some of the unusual cascades of border collision bifurcations that are involved in the transitions from stable period-1 dynamics to chaos in a single-phase pulse-width modulated H-bridge inverter.

### 2. Non-autonomous piecewise-smooth map

The dynamics of our single-phase H-bridge inverter may be represented by the following non-autonomous piecewise-smooth 1D map:

$$x_{k+1} = F(x_k, k), \quad k = 0, 1, 2, \dots \quad (1)$$

with

$$F(x_k, k) = \begin{cases} F_L(x_k) = e^\lambda(x_k + 1) + 1, & \text{if } x_k \leq s_k^-; \\ F_M(x_k) = e^\lambda(x_k - 1) + 2e^{\lambda(1-z_k)} - 1, & \text{if } s_k^- < x_k < s_k^+; \\ F_R(x_k) = e^\lambda(x_k - 1) - 1, & \text{if } x_k \geq s_k^+, \end{cases} \quad (2a)$$

$$s_k^\pm = \frac{q}{\Gamma} \cos\left(\frac{2\pi k}{m}\right) \pm \frac{P}{\alpha\Gamma}, \quad (2b)$$

$$z_k = \alpha \cos\left(\frac{2\pi k}{m}\right) - \frac{\alpha\Gamma}{2P}x_k + \frac{1}{2}. \quad (2c)$$

A detailed description of the inverter circuit, the functioning of the inverter, and its areas of application can be found in [5, 6]. Here, one can also find an explanation of the model equations and the description of the method used to derive the map (1).

The (dimensionless) dynamic variable  $x$  is the normalized load current and  $k = 1, 2, \dots$  represents the normalized discrete time variable. Hereby  $x_k$  denotes the value of the dynamic variable  $x$  at the discrete time  $k$  (switching time), and the auxiliary variable  $z_k \in [0, 1]$  represents the relative pulse duration in the  $k$ th ramp cycle.

The parameter  $\lambda = -1/\tau_*$  is defined by the time constant  $\tau_*$  of the converter filter, normalized relative to the ramp period. The parameter  $P$  controls the amplitude of the ramp function,  $q$  represents the normalized amplitude of the sinusoidal reference signal. The parameter  $\alpha$  is an amplification constant and  $\Gamma$  is the normalized input voltage to the inverter.

The value  $m = T/a$  is referred to as the frequency modulation ratio, where  $a$  and  $T$  denote, respectively, the ramp period and the period of the reference sinusoidal signal. It

is worth to emphasize that the value of  $m$  influences directly the quality of the output sinusoidal signal. To obtain an output signal with a low-distortion, it is necessary to use a high value of  $m$ .

The normal operational regime for DC/AC converters is the stable period-1 dynamics. Under normal operation, sufficiently low-distortion for the output signal can usually be achieved through the choice of parameters for the output filter (value of  $\tau_*$ ) or the feedback corrector. However, increasing the value of the corrector feedback gain  $\alpha$  in order to attain a more accurate control may lead to loss of stability for the period-1 mode and to the appearance of sub-harmonic or chaotic oscillations. Such dynamics leads to distortions of the output signal.

In the following simulations we have chosen  $P = 20.0$ ;  $q = 40.0$ ;  $\lambda = -0.2$ ;  $m = 100$ . The corrector gain factor  $\alpha$  and the normalized input voltage  $\Gamma$  are used as the main control parameters:  $\alpha > 0$ ,  $25.0 < \Gamma < 60.0$ .

### 3. Autonomous stroboscopic map

Clearly, the non-autonomous 1D map (1) can easily be transformed into a 2D autonomous map. Moreover, as the cosine function in Eq. (2) is  $m$ -periodic, for any  $x$  the equality

$$F(x, k) = F(x, k + m)$$

is satisfied. Therefore, the  $m$ th iterate

$$\begin{aligned} x_{k+1} &= f^m(x_k) \\ &= F(F(\dots F(F(x_k, 0), 1) \dots), m-2), m-1) \end{aligned} \quad (3)$$

represents a 1D stroboscopic map for the 2D autonomous variant of map (1) which completely reflects the dynamics of map (1).

To understand the properties of map (3) it is worth noticing that for each fixed  $k \in \{0, \dots, m-1\}$  the function  $F(x, k)$  is a continuous piecewise-smooth bimodal function. On the two outer partitions (i.e. for  $x_k \leq s_k^-$  and for  $x_k \geq s_k^+$ ) the function  $f$  is defined by linearly increasing branches  $F_L$ ,  $F_R$ , whereas on the middle partition, i.e. for  $s_k^- < x_k < s_k^+$  it has a non-linear decreasing branch  $F_M$ . As the function  $f^m$  results from iterated applications of continuous piecewise-smooth functions  $F(x, k)$ ,  $k = 0, \dots, m-1$ , it represents a continuous piecewise-smooth function as well. However, the number of border points of  $f^m$  may be very high. Indeed, these border points are given by the border points  $s_k^\pm$ ,  $k = 0, \dots, m-1$  of  $F$  and by their preimages. Therefore, depending on other parameters, the number of border points of this map may grow exponentially with increasing  $m$ .

Note that the stable period-1 dynamics corresponding to the normal operational regime of the considered class of converter systems is represented in map (3) by a stable fixed point. Accordingly, our goal is reduced now to the investigation of the stability domains of the fixed points of map (3) and in particular of its boundary.

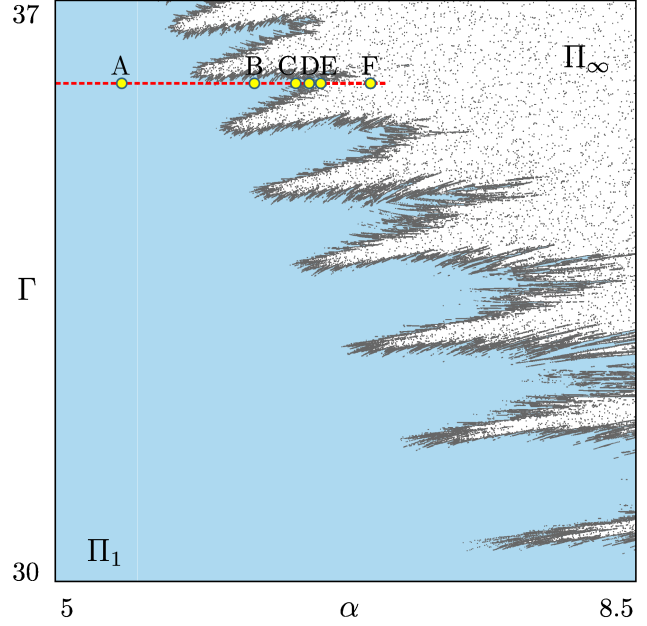


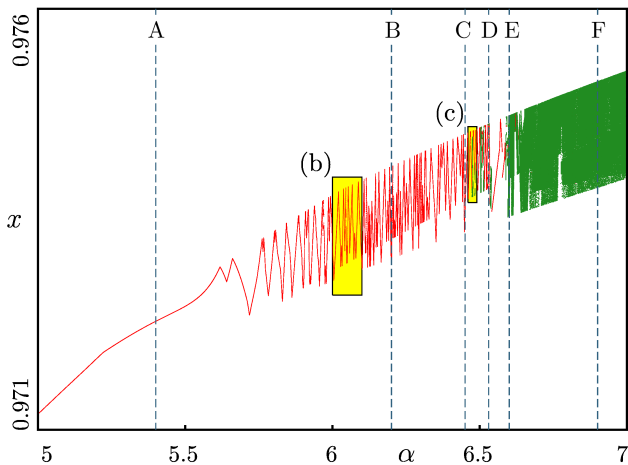
Figure 1: Bifurcation structure of the  $(\alpha, \Gamma)$ -parameter plane of map (3). The stability domain of the fixed point and the domain of chaotic dynamics are denoted by  $\Pi_1$  and  $\Pi_\infty$ , respectively. The bifurcation diagram along the horizontal line marked at  $\Gamma = 36$  is shown in Fig. 2. The functions  $f^m$  at the parameter values marked with A – F are shown in Figs. 3(a) – (f), respectively.

### 4. Bifurcation structure

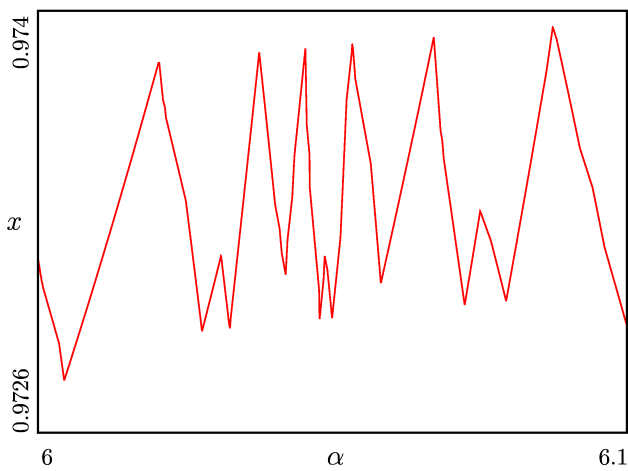
Fig. 1 shows an example of the bifurcation structure that can be observed in the  $(\alpha, \Gamma)$ -parameter plane of map (3). The most striking feature of this figure is the unusual form of the boundary between the stability domain of the fixed point  $\Pi_1$  and the domain of chaotic dynamics  $\Pi_\infty$ . Indeed, a direct transition from a stable fixed point to chaos via a border collision bifurcation is a well-known phenomenon in piecewise-smooth systems. Still, the questions arise why the boundary between  $\Pi_1$  and  $\Pi_\infty$  has such a frayed shape and which the bifurcations are that cause this structure.

In order to examine these questions let us consider a 1D bifurcation diagram showing the transition from  $\Pi_1$  to  $\Pi_\infty$ . An example for such a diagram is illustrated in Fig. 2. In this diagram, three zones can clearly be distinguished.

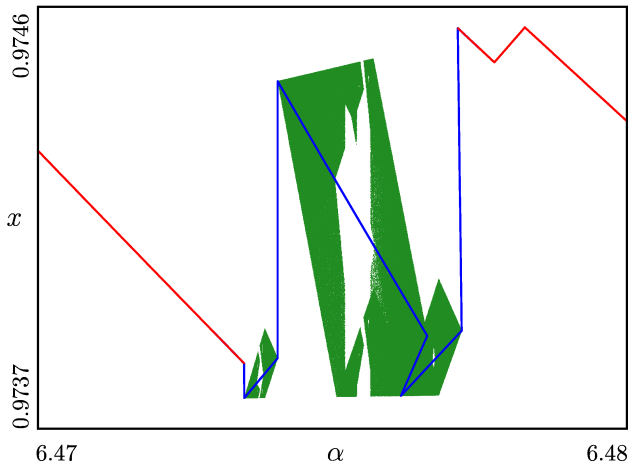
- (i) In the left part of the bifurcation diagram the fixed point is stable. As already mentioned, this corresponds to the desired dynamics of the converter.
- (ii) In the right part of the bifurcation diagram the map shows chaotic behavior. Clearly, for the modeled converter this mode of operation is not acceptable.
- (iii) In the middle part of the bifurcation diagram, the attractor of the map is still given by a stable fixed point. However, the location of this fixed point in the phase space is strongly dependent on the parameter which is clearly reflected in the oscillations of the bifurcation diagram. For



(a)



(b)



(c)

Figure 2: Transition from a stable fixed point to chaos via a cascade of border collision bifurcations. Rectangles marked in (a) are drawn enlarged in (b) and (c). Stable fixed points are shown red, unstable fixed points blue, chaotic attractors green. The functions  $f^m$  at the parameter values marked in (a) with A – F are shown in Figs. 3(a) – (f), respectively.  $\Gamma = 36$ .

increasing  $\alpha$  these oscillations become more and more strong so that in a practical situation a small fluctuation of the parameters leads to a significant change of the output signal. Hence, the dynamics is not robust in this parameter region.

As one can see in the enlargement shown in Fig. 2(b), in extended parameter ranges the only asymptotic dynamics of map (3) is given by a stable fixed point. However, this fixed point undergoes a sequence of bifurcations causing it to oscillate in an irregular manner in dependency on  $\alpha$ . Moreover, as shown in Fig. 2(c), for increasing  $\alpha$  the fixed point can be destabilized and eventually restabilized again. When the fixed point is unstable, other attractors of map (3) appear, in particular chaotic. The question is now, which mechanism leads to these phenomena.

To explain the observed cascades of bifurcations let us consider how the shape of the function  $f^m$  changes when the parameters are varied along a path which leads from  $\Pi_1$  to  $\Pi_\infty$ . An example corresponding to the bifurcation diagram shown in Fig. 2 is illustrated in Fig. 3. As one can see, for increasing  $\alpha$  the function moves upwards, but this movement is marginal. The main effect of the increasing  $\alpha$  is the decrease of the distance between the border points of  $f^m$ . Note that far away from the boundary between  $\Pi_1$  and  $\Pi_\infty$  (see Fig. 3(a)) the complete portion of the phase space shown in Fig. 3 contains only one branch of  $f^m$ . Hereby the slope of this branch is close to zero.<sup>1</sup> For increasing  $\alpha$ , the distance between the border points of  $f^m$  decreases (see Fig. 3(b)), so that the fixed point moves from one branch of  $f^m$  to the next one. Therefore, the bifurcations forming the cascades described above are border collision bifurcations. Clearly, as long as the slopes of the branches, to which the fixed point belongs before and after the bifurcations, do not exceed one in modulus, these border collisions are not associated with a loss of stability of the fixed point (accordingly, we can not observe them in Fig. 1). Following the wide-spread terminology [7], these bifurcations are referred to as persistence border collisions. Accordingly, we classify the oscillations of the stable fixed point which are clearly visible in the bifurcation diagram (see Fig. 2) as cascades of persistence border collisions.

With increasing  $\alpha$ , as the border points of  $f^m$  move closer to each other, it may also happen that the slopes of some of the branches of  $f^m$  exceed one in modulus, while the slope of other branches are still less than one in modulus (see Figs. 3(c) and (d)). For simplicity, we denote the branches of first kind as stable and of the second ones as unstable. In this case, as the fixed point reaches an unstable branch, it is momentarily destabilized, but eventually, for further increasing values of  $\alpha$  it reaches a stable branch and is restabilized again, as shown in Fig. 2(c). As long as the fixed point belongs to an unstable branch, the map

<sup>1</sup>Speaking rigorously, the term “slope” can not be applied to branches of  $f^m$ , as they are given by nonlinear functions. Still, for simplicity of the exposition we use this term, as at the considered parameter values the branches of  $f^m$  are almost linear.

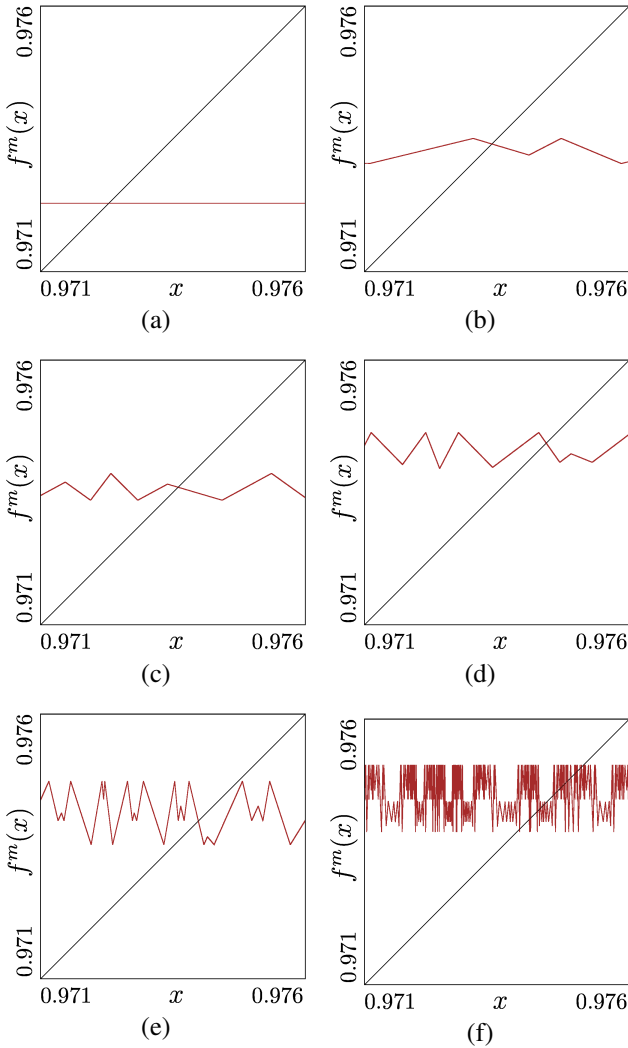


Figure 3: Shape of the function  $f^m$  close to its intersection with the diagonal at  $\Gamma = 36$  and (a)  $\alpha = 5.4$ ; (b)  $\alpha = 6.2$ ; (c)  $\alpha = 6.45$ ; (d)  $\alpha = 6.53$ ; (e)  $\alpha = 6.6$ ; (f)  $\alpha = 6.9$ .

has other attractors, which are either harmonic  $2^k$ -cycles,  $k = 1, 2, \dots$ , or chaotic attractors. As shown in [6], these attractors may undergo further bifurcations (in particular, merging and final bifurcations, see [8] for details), and may coexist.

With  $\alpha$  further increasing, the border points of  $f^m$  continue to move closer to each other, so that the number of stable branches decreases and the number of unstable branches increases. For example, in Fig. 3(e) only a few stable branches can be observed. Accordingly, the parameter intervals in the bifurcation diagram associated with chaotic attractors grow, and the intervals associated with the stable fixed point vanish. Finally, all the branches of  $f^m$  become unstable (see Fig. 3(f)) and the map shows chaotic dynamics only.

## 5. Conclusion

The paper has presented an example of a new type of complex dynamics in a power electronic DC/AC converter, caused by the presence of two internal oscillatory modes (the ramp cycle and the external reference signal). We considered a model of a single-phase H-bridge inverter with pulse-width modulated control. The behavior of this inverter is described by a non-autonomous piecewise-smooth map. The normal operational regime for such converters is the regime of stable period-1 dynamics, corresponding to a stable fixed point of the one-dimensional autonomous stroboscopic map (3). We have shown that, under variation of the parameters, this stable fixed point undergoes an unusual sequence of border collision bifurcations that gives birth to different forms of chaotic dynamics. The observed bifurcation phenomena differ essentially from the well-known direct transition from a stable fixed point to chaos frequently occurring in piecewise-smooth maps.

## Acknowledgments

V. Avrutin was supported by the European Community within the scope of the project “Multiple-discontinuity induced bifurcations in theory and applications” (Marie Curie Action of the 7th Framework Programme, Contract Agreement N. PIEF-GA-2011-300281).

## References

- [1] M. H. Rashid and F. L. Luo, editors. *Power Electronics Handbook*. Elsevier Science, 2006.
- [2] M.P. Kazmierkowski, R. Krishnan, and F. Blaaberg. *Control in Power Electronics - Selected Problems*. Elsevier Science, 2002.
- [3] V. Anishchenko, S. Nikolaev, and J. Kurths. Winding number locking on a two-dimensional torus: Synchronization of quasiperiodic motions. *Phys. Rev. E*, 73:056202, 2006.
- [4] J. L. Laugesen, E. Mosekilde, and N.-H. Holstein-Rathlou. Synchronization of period-doubling oscillations in vascular coupled nephrons. *Chaos*, 21:033128, 2011.
- [5] Zh. T. Zhusubaliyev, E. Mosekilde, A. I. Andriyanov, and V. V. Shein. Phase synchronized quasiperiodicity in power electronic inverter systems. *Physica D*, 268:14–24, 2014.
- [6] V. Avrutin, Zh. T. Zhusubaliyev, E. Mosekilde, and L. Gardini. Onset of chaos in a single-phase power electronic inverter. *In preparation*, 2014.
- [7] M. di Bernardo, C. J. Budd, A. R. Champneys, and P. Kowalczyk. *Piecewise-smooth Dynamical Systems: Theory and Applications*, volume 163 of *Applied Mathematical Sciences*. Springer, 2008.
- [8] V. Avrutin, L. Gardini, M. Schanz, and I. Sushko. Bifurcations of chaotic attractors in one-dimensional maps. *Int. J. Bifurcat. Chaos*, 2014. (accepted for publication).